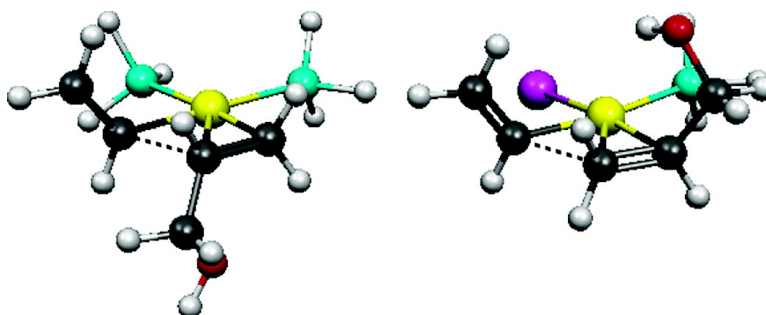


Electronic Control of the Regiochemistry in Palladium–Phosphine Catalyzed Intermolecular Heck Reactions

Robert J. Deeth, Andrew Smith, and John M. Brown

J. Am. Chem. Soc., **2004**, 126 (22), 7144-7151 • DOI: 10.1021/ja0315098 • Publication Date (Web): 14 May 2004

Downloaded from <http://pubs.acs.org> on March 31, 2009



More About This Article

Additional resources and features associated with this article are available within the HTML version:

- Supporting Information
- Links to the 7 articles that cite this article, as of the time of this article download
- Access to high resolution figures
- Links to articles and content related to this article
- Copyright permission to reproduce figures and/or text from this article

[View the Full Text HTML](#)

Electronic Control of the Regiochemistry in Palladium–Phosphine Catalyzed Intermolecular Heck Reactions

Robert J. Deeth,* Andrew Smith, and John M. Brown†

Contribution from the Inorganic Computational Chemistry Group, Department of Chemistry, University of Warwick, Coventry CV4 7AL, UK

Received December 4, 2003; E-mail: r.j.deeth@warwick.ac.uk

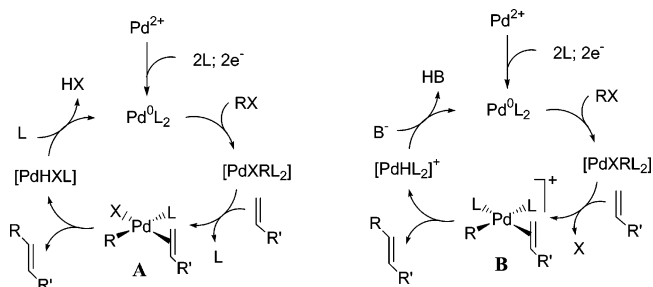
Abstract: Density functional theory calculations of the transition-state structures and reaction barriers for the C–C coupling between monosubstituted η^2 -olefins and η^1 -vinyl for neutral $[\text{Pd}(\text{PH}_3)(\text{vinyl})(\text{RCHCH}_2)]$ and cationic $[\text{Pd}(\text{H}_2\text{PCH}_2\text{PH}_2)(\text{vinyl})(\text{RCHCH}_2)]^+$ ($\text{R} = \text{OMe}, \text{Me}, \text{and CN}$) depend mostly on the regiochemistry and not on the starting position of the olefin substituent. The regiochemistry is thus implicit in the *electronic* structure of the precursor complex. A selectivity index, Ω , based on electrostatic and frontier orbital interactions gives a good correlation with experiment for vinylations or arylations. The model correctly predicts that the regiochemistry for $\text{R} = \text{OMe}, \text{Me}, \text{and CN}$ is the same for both neutral and cationic Pd complexes while for $\text{R} = \text{CH}_2\text{OH}$ the regiochemistry reverses. The latter is confirmed by explicit calculations of the transition-state energies. Selectivity indices are computed for 13 substituents: $\text{CO}_2\text{Me}, \text{CN}, \text{CF}_3, \text{Ph}, \text{H}, \text{Me}, \text{CH}_2\text{OH}, \text{CH}_2\text{NMe}_2, 2\text{-pyrrolidone}, \text{CH}_2\text{SiMe}_3, \text{OAc}, \text{OMe}, \text{and F}$. Cationic conditions systematically give larger Ω values and thus tend to favor coupling at the α carbon on the olefin. The Ω values are approximately additive and can be used to predict the regiochemistry for disubstituted olefins.

Introduction

The Heck reaction^{1,2} is one of the most versatile methods for generating new carbon–carbon bonds.^{3–6} Using Pd-based catalysts, the reaction couples an unsaturated carbon center, often from a vinyl or aryl group, to one end of an alkene C=C bond. Both inter- and intramolecular examples are known.

Heck chemistry occurs under diverse conditions and catalysts. High temperature/high turnover systems involve a palladocycle which reversibly liberates the true catalyst, while the phosphine-free conditions developed by Jeffery^{7,8} almost certainly involve Pd nanoparticles. For less exotic circumstances, the qualitative ideas about the regiochemistry of intermolecular Heck coupling have been reviewed by Cabri.⁹ Depending on the conditions, the Heck reaction is believed to follow one of the two different mechanisms shown in Scheme 1. Despite suggestions of a mechanism involving Pd(IV) species,¹⁰ the consensus appears to be that Heck reactions involve a Pd^{0/II} couple.

Scheme 1. Simplified Scheme for “Neutral” (Left) and “Cationic” (Right) Heck Reactions



In Scheme 1, the first step involves the oxidative addition of an aryl or vinyl halide or triflate, RX, to a Pd(0) species, which normally contains auxiliary donors, L, where L is often a phosphine. This step may be preceded by a reduction of the metal if a Pd(II) salt is employed initially. Thereafter, the pathways are distinguished by which group dissociates to provide a vacant coordination site for the incoming alkene. If a phosphine ligand detaches and the halide is retained, the active species immediately prior to the C–C coupling step is the neutral complex $[\text{PdXLR}(\text{alkene})]$, **A**. Conversely, if X^- is removed (say by addition of a silver salt if $\text{X}^- = \text{halide}$), the active species is the cationic complex $[\text{PdRL}_2(\text{alkene})]^+$, **B**.

The latter “cationic” (or polar) pathway can be further favored by the use of a bidentate auxiliary ligand, and asymmetric versions of the Heck reaction have been developed using well-

† Current address: Chemistry Research Laboratory, University of Oxford, Mansfield Rd., Oxford OX1 3TA, UK.

- Heck, R. F. In *Comprehensive Organic Synthesis*; Trost, B. M., Fleming, I., Eds.; Pergamon Press: Oxford, 1991; Vol. 4.
- Heck, R. F. *J. Am. Chem. Soc.* **1969**, *91*, 6707.
- Beletskaya, I. P.; Cheprakov, A. V. *Chem. Rev.* **2000**, *100*, 3009–3066.
- Shibasaki, M.; Vogl, E. M. *J. Organomet. Chem.* **1999**, *576*, 1–15.
- Demeijere, A.; Meyer, F. E. *Angew. Chem., Int. Ed. Engl.* **1995**, *33*, 2379–2411.
- Crisp, G. T. *Chem. Soc. Rev.* **1998**, *27*, 427–436.
- Jeffery, T. *Adv. Met.-Org. Chem.* **1996**, *5*, 153–260.
- Jeffery, T.; Galland, J. C. *Tetrahedron Lett.* **1994**, *35*, 4103–4106.
- Cabri, W.; Candiani, I. *Accounts Chem. Res.* **1995**, *28*, 2–7.
- Sundermann, A.; Uzan, O.; Martin, J. M. L. *Chem.-Eur. J.* **2001**, *7*, 1703–1711.

known bidentate phosphines such as BINAP¹¹ which generates the familiar C₂-symmetry motif common in asymmetric chemistry.

As with many catalytic processes, defining the scope and utility of the Heck reaction has proceeded largely through trial and error.^{6,12} In the case of the intermolecular Heck reaction, the regiochemistry is reported to depend on both the reaction conditions (i.e., “neutral” versus “cationic” pathways) and the alkene substituents.⁹ Under “neutral” reaction conditions, aryl groups attack the β carbon of monosubstituted alkenes, leading to the suggestion that the process is controlled by steric interactions. Under “cationic” conditions, the site of attack varies with the alkene substituent. It is supposed that the alkene bond is more polarized in the cationic species **B** and hence more susceptible to electronic effects from the substituents. Electron-donating substituents activate the α carbon thus favoring internal olefins, while electron-withdrawing groups activate the β carbon leading to terminal olefins.

These general conclusions need to be interpreted with care since they are based on relatively limited examples which can themselves depend on the reaction conditions. Thus, despite the many successful applications of Heck chemistry, many problems remain. Indeed, Beletskaya and Cheprakov go so far as to assert “we cannot make any predictions about the regiochemistry of arylation ... and temptations to find simple rules should be discarded.”³ Such a challenge is irresistible to the computational chemist, and we have thus set about modeling the Heck reaction in detail to establish the validity of their assertion.^{11,13} We report here an extensive series of density functional theory (DFT) calculations which lead to a numerical selectivity index which correctly predicts the regiochemistry for coupling of a vinyl (or aryl) group to a monosubstituted alkene and provides both a basis for ranking substituents in order of their increasing tendency to direct the incoming group to either the α or β positions on the olefin and a procedure for computing the behavior of substituents we have not yet considered.

DFT has revolutionized the accurate theoretical treatment of transition metal systems and provides a viable theoretical tool for probing intimate mechanistic details. Albert et al.¹⁴ have reported a study of the Heck reaction between phenyl and ethylene using imines as ligands while von Schenck et al.¹⁵ and Ludwig et al.¹⁶ report computational results on di-imine and mixed N,O and O,P donors. The present study complements the other studies in that we consider a wide range of olefin substituents but only sterically undemanding phosphines as auxiliaries while, in particular, Schenck et al.¹⁵ focused on one olefin, propene, but explored the regiochemical effects of a range of auxiliary co-ligands.

Phosphines are commonly used experimentally, and we presented a preliminary account describing the model cationic Heck reaction comprising the coupling of a methyl group to ethylene.¹³ This study was limited to the reaction of base with a late catalytic intermediate and established the greater acidity

of an agostic C–H over a normal β -alkyl C–H. It was also useful in establishing the basic computational protocols. However, since CH₃ is not competent in Heck chemistry, our first goal is to extend the modeling to include the practically more realistic vinyl group. The second goal is to examine in detail the effect of alkene substituents on the regiochemistry of the intermolecular Heck reaction for both neutral and cationic pathways.

Computational Details

The DFT calculations were obtained using the Amsterdam density functional (ADF) program suite versions 2000.02.¹⁷ and 2003.01. Geometries and frequencies were generally obtained using the local density approximation (LDA)¹⁸ although the gradient-corrected Becke88/Perdew86 functional (BP86)^{19,20} was also used to compare the effect on the calculated structures. Total binding energies were calculated at the BP86 level. The frozen-core approximation²¹ was applied with orbitals 1s–3d frozen on Pd, 1s–2p on P and S, 1s–4d on I, and the 1s orbital on O, N, and C. Basis sets comprised triple- ζ + polarization STO expansions (basis IV) on all centers. Default criteria were employed throughout. All transition-state structure optimizations reported a single negative Hessian eigenvalue. Given the close similarities in TS structures, confirmatory frequency calculations were only deemed necessary for a few representative examples as described in the text.

Results and Discussion

At the start of this project, all structures were computed at the LDA level with single-point BP86 energies. This choice was partly due to computational efficiency—LDA calculations are about three times faster than BP86 optimizations—and partly due to our experience with relatively ionic coordination complexes which showed that LDA-optimized metal–ligand distances are in better agreement with experiment than those from gradient-corrected functionals.²² However, this observation does not extend to more covalent organometallic compounds such as the metal carbonyls where the well-documented tendency for the LDA to overbind manifests as too short M–L distances.²³ Even if the metal center would normally be described as hard–Co(III) for instance—and thus well suited to the LDA, if the ligands are sufficiently soft, the LDA predicts M–L bond lengths which are too short as is the case in CoX₃–(LR₃)₂ complexes where X = Cl, Br, I, and L = P, As, Sb.²⁴

However, it is also clear that it is far more important to get the energetics right than to insist on very accurate structures. Siegbahn, for example, advocates optimizing structures using rather small basis sets to save computer time which can give “errors” in M–L bond lengths up to 0.1 Å.²⁵ However, since

- (11) Hii, K. K.; Claridge, T. D. W.; Brown, J. M.; Smith, A.; Deeth, R. J. *Helv. Chim. Acta* **2001**, *84*, 3043–3056.
- (12) Soderberg, B. C. G. *Coord. Chem. Rev.* **2002**, *224*, 171–243.
- (13) Deeth, R. J.; Smith, A.; Hii, K. K.; Brown, J. M. *Tetrahedron Lett.* **1998**, *39*, 3229–3232.
- (14) Albert, K.; Gisdakis, P.; Rosch, N. *Organometallics* **1998**, *17*, 1608–1616.
- (15) von Schenck, H.; Akermark, B.; Svensson, M. *J. Am. Chem. Soc.* **2003**, *125*, 3503–3508.
- (16) Ludwig, M.; Stromberg, S.; Svensson, M.; Akermark, B. *Organometallics* **1999**, *18*, 970–975.

- (17) Baerends, E. J.; Bérces, A.; Bo, C.; Boerrigter, P. M.; Cavallo, L.; Deng, L.; Dickson, R. M.; Ellis, D. E.; Fan, L.; Fischer, T. H.; Fonseca Guerra, C.; van Gisbergen, S. J. A.; Groeneveld, J. A.; Gritsenko, O. V.; Harris, F. E.; van den Hoek, P.; Jacobsen, H.; van Kessel, G.; Kootstra, F.; van Lenthe, E.; Osinga, V. P.; Philipsen, P. H. T.; Post, D.; Pye, C. C.; Ravenek, W.; Ros, P.; Schipper, P. R. T.; Schreckenbach, G.; Snijders, J. G.; Sola, M.; Swerhone, D.; te Velde, G.; Vernooijs, P.; Versluis, L.; Visser, O.; van Wezenbeek, E.; Wiesenekker, G.; Wolff, S. K.; Woo, T. K.; Ziegler, T.; *Scientific Computing and Modelling NV*; Free University: Amsterdam, 2000.
- (18) Slater, J. C. *Adv. Quantum Chem.* **1972**, *6*, 1.
- (19) Becke, A. D. *Phys. Rev. A* **1988**, *38*, 3098–3100.
- (20) Perdew, J. P. *Phys. Rev. B, Condensed Matter* **1986**, *33*, 8822–8824.
- (21) Baerends, E. J.; Ellis, D. E.; Ros, P. *Theor. Chim. Acta* **1972**, *27*, 339.
- (22) Bray, M. R.; Deeth, R. J.; Paget, V. J.; Sheen, P. D. *Int. J. Quantum Chem.* **1997**, *61*, 85–91.
- (23) Li, J.; Schreckenbach, G.; Ziegler, T. *J. Phys. Chem. B* **1994**, *98*, 4838–4841.
- (24) Deeth, R. J. *J. Chem. Soc., Dalton Trans.* **1997**, 4203–4207.
- (25) Siegbahn, P. E. M. *J. Comput. Chem.* **2001**, *22*, 1634–1645.

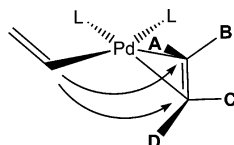


Figure 1. Possible regiochemistry as a function of substituent position.

Table 1. Relative Binding Energies (BP86, kJ mol^{-1}) for Each Substituent Position Shown in Figure 1 for $R = \text{Me}$, CN , and OMe

substituent position	$R = \text{Me}$	$R = \text{CN}$	$R = \text{OMe}$
A	3.1	6.7	6.7
B	0.5	0.0	1.2
C	0.0	0.5	0.0
D	2.7	5.3	9.8

all stationary points are located using the same level of theory, there is substantial cancellation of errors, and subsequent single-point calculations of the energies using larger basis sets yield reliable profiles of the reaction paths.

We adopt the same philosophy here, and while we acknowledge that the LDA-optimized structures will have slightly shorter bond lengths than BP86 structures, the differences are relatively small (typically a few hundredths of an Å) and will not have a significant impact on the relative energetics.

The starting model system comprises a cationic palladium–methylenediphosphine fragment to which vinyl and alkenes are coordinated. A single alkene substituent can occupy one of four different positions as shown in Figure 1. Although the vinyl group could also be oriented below the coordination plane, the unsubstituted methylenediphosphine auxiliary ligand ensures that this would simply generate the four matching optical isomers.

Optimized geometries and relative binding energies were computed for all four possibilities for each of the three substituents $R = \text{Me}$, CN , and OMe (Table 1). Positions **B** and **C** correspond to the substituent oriented away from the vinyl group and, for a given R , have virtually identical energies and bond lengths. Positions **A** and **D** orient the substituent toward the vinyl group which presumably explains why the energies increase relative to sites **B** and **C**.

The particular lowest energy structures for $R = \text{Me}$, CN , and OMe correspond to substituent positions **C**, **B**, and **C**, respectively, and are shown in Figure 2. The structures are generally very similar. The $\text{Pd}-\text{C}_{\text{vinyl}}$ distances are all 2.01 Å. The vinyl exerts a much stronger trans influence with the trans $\text{Pd}-\text{P}$ distance between 2.44 and 2.46 Å versus a $\text{Pd}-\text{P}$ bond length of 2.31 Å trans to the alkene. Predictably, the biggest differences concern the alkene binding where the $\text{Pd}-\text{C}_{\alpha}$ and $\text{Pd}-\text{C}_{\beta}$ bonds are 2.30 and 2.23 Å, 2.25 and 2.26 Å, and 2.40 and 2.19 Å for the three substituents, respectively. Note that the substituent at the C_{α} position tends to give a longer bond to the Pd for $R = \text{CH}_3$. The electron-withdrawing CN group counters this effect while the OMe group enhances it. Also, in common with Rh complexes, alkoxyalkene coordination to Pd stabilizes the *trans* arrangement of the OMe group compared to the *cisoid* structure of the isolated alkene.²⁶

For each of the four substituent positions, there are two possible sites of attack shown by the arrows in Figure 1 generating a total of eight reaction paths. Four will lead to linear product corresponding to attack at the β carbon and four to

branched product (α carbon attack). Within each set of four, only two unique pathways would be expected, one corresponding to the vinyl groups and the alkene substituent being mutually cis and one where they are mutually trans. However, this requires that the metal, the donor atoms, and their associated four-membered rings are coplanar. Due to the puckering of the four-membered $\text{P}-\text{Pd}-\text{P}-\text{C}$ and $\text{Pd}-\text{C}-\text{C}-\text{C}$ rings (Figure 3), each of the four possible pathways is different and we have explicitly computed them all.

Preliminary linear transit calculations where the constrained variable was the distance between the coordinated vinyl carbon, C_{vin} , and one of the olefin carbons (C_{α} or C_{β}) revealed the preferred reaction pathway rotated the alkene into the square plane, as we found before,^{11,13} and that the $\text{C}-\text{C}$ distance at the transition state (TS) was around 2–2.1 Å. Accordingly, the nearest structure was employed in a full TS search. In all cases, the program converged, reporting a single negative eigenvalue in the Hessian matrix. Frequency calculations were carried out for the lowest energy β -attack TSs for $R = \text{Me}$ and $R = \text{OMe}$ and for the α -attack TS for $R = \text{Me}$. In all cases, a single imaginary frequency of about -300 cm^{-1} resulted, confirming that the program had successfully located a first-order saddle point. Animation of this mode revealed the dominant motion was the change of the $\text{C}_{\text{vin}}-\text{C}_{\alpha/\beta}$ distance. The ADF program computes vibrations via numerical differentiation of analytical first derivatives which, with two displacements for each degree of freedom, requires up to about 150 evaluations per molecule. This, coupled with the higher integration level required for reasonable accuracy, results in excessively long calculations. Hence, we have not formally verified every single TS structure, but given that all the systems considered here are so similar, we are confident that all the TS structures are satisfactory.

Assuming easy interconversion, the energetic data in Table 1 suggest there should be mixtures of reactant species corresponding to the substituent placed at various positions but mostly at **B** or **C**. However, taking the Curtin–Hammett postulate, each reaction proceeds via the lowest energy TS irrespective of the initial substituent position. Hence, the theoretical selectivity depends on the difference, $\Delta\Delta E^{\ddagger}$, between the lowest energy TS leading to linear product and the lowest energy TS leading to branched product.

The calculated reaction barriers (relative to the *overall* lowest energy structure for each R in Table 1) are shown in Figure 4. The data are not corrected for zero-point motions nor the effects of temperature, but these corrections are expected to cancel out. The structures and bond lengths for the lowest energy TSs are depicted in Figure 5 along with the energy of the branched pathway TS relative to the linear pathway.

The calculations predict that for $R = \text{Me}$ the selectivity is low (the two competing TSs differ by on 1 kJ mol^{-1}), for $R = \text{CN}$ β -attack is favored (linear product TS favored by 16 kJ mol^{-1}) [This conclusion was tested for $R = \text{CN}$ using the BP86 functional for both geometries and energies. The forming $\text{C}-\text{C}$ bond length increases by about 0.04 Å relative to the LDA structures and the linear pathway TSs is favored by about 8 kJ mol^{-1} more (i.e., the energy difference between TSs increases to about 24 kJ mol^{-1}).], and for $R = \text{OMe}$ α -attack is favored (branched product TS favored by 9 kJ mol^{-1}).

The observed regiochemistry of experimental Heck coupling depends strongly on the olefin substituent R . Under cationic

(26) Price, D. W.; Drew, M. G. B.; Hii, K. K.; Brown, J. M. *Chem.-Eur. J.* **2000**, *6*, 4587–4596.

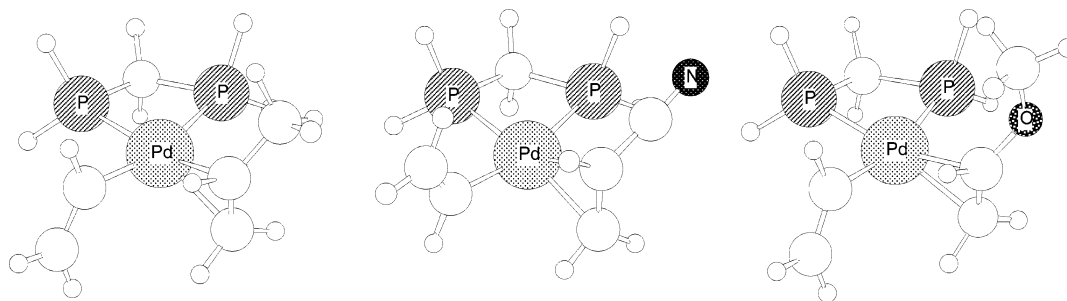


Figure 2. Optimized structures for the lowest energy configurations for each substituent.

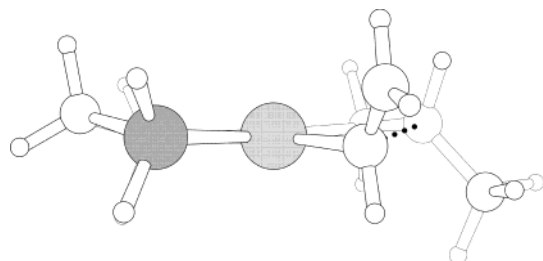


Figure 3. Side view of optimized TS structure for branched pathway, R = CH₃, showing slight puckering of phosphine chelate and vinylalkene rings.

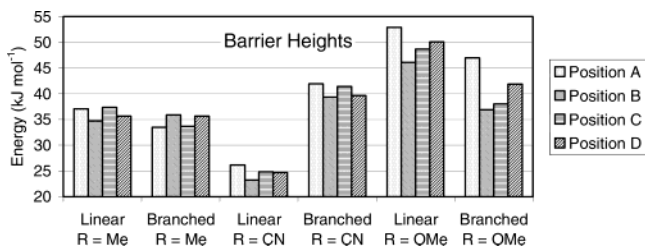


Figure 4. Calculated barrier heights relative to lowest energy structures in Table 1.

coupling conditions with aryl triflates or halides plus TI⁺, product ratios are observed corresponding to 100% β -attack for R = CN through intermediate product distributions for R = alkyl to \sim 95% α -attack for R = OMe. Hence, the theoretical predictions correlate very well with experiment. Note that the present calculations are based on a diphosphine catalyst while some of the experimental data refer to different ligand systems. However, calculations on related diamine and mixed amino-phosphine species give qualitatively similar results to those for diphosphine species.²⁷

Another important feature of the calculations is that the $\Delta\Delta E^\ddagger$ values only fluctuate by \sim 5 kJ mol⁻¹ as a function of substituent position. Hence, notwithstanding the Curtin-Hammett principle, the predicted selectivity is relatively insensitive to substituent position. Given the simple model systems used here, it is gratifying to get such good agreement with experiment. Of course, since the critical issue is the energy difference between two relatively similar TSs, significant cancellation of errors can be expected.

The calculated and observed regioselectivity for the cationic pathway is consistent with the substituent electronic effects in the isolated alkene. Thus, since CN is electron-withdrawing, the unsubstituted carbon is activated toward nucleophilic attack while, conversely, OMe can act in an electron-donating fashion which activates the substituted carbon. For the cationic mech-

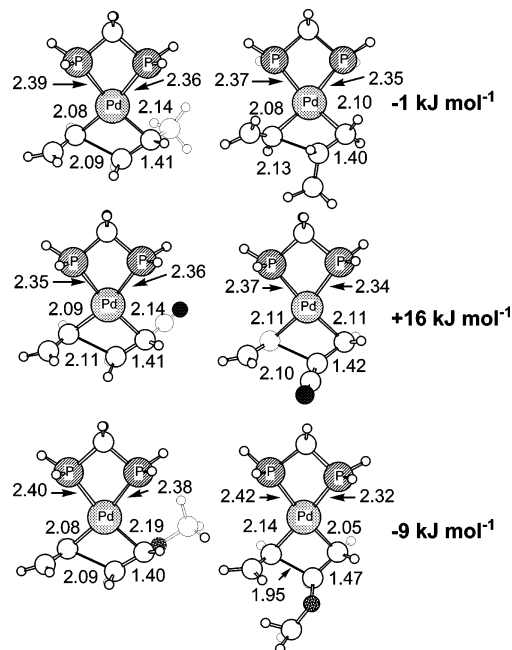


Figure 5. Lowest energy transition-state optimized structures leading to either linear (left) or branched (right) product. The numerical values on the right are the energies of the branched TS relative to the linear TS.

anism, the basic electronic structure of the alkene is apparently preserved on coordination to the palladium and electronic effects direct the regiochemistry.

In contrast, the observed regiochemistry for neutral reactions usually favors linear products which has been interpreted as implying the regiochemistry is determined mainly by steric interactions.⁹ However, for R = OMe, there is still greater than 60% branched product while substituents with a hydroxyl group can show complete reversal. For R = CH(OH)Me, for example, a cationic pathway leads to 100% branched product while the neutral pathway gives 100% linear product. Assuming the mechanism remains unchanged, these observations argue for an electronic basis to the selectivity. If true, then theory should correctly predict those R groups where the regiochemistry changes with the reaction conditions and those where it remains the same.

To investigate this, we follow a similar procedure to that outlined above for neutral pathway reactions with R = CN and OMe. Using PH₃ as a model phosphine, iodide as the halide ligand (cis to vinyl), and placing the R group in position C, transition states for both linear and branched pathways were optimized. For R = CN the TS leading to linear product is favored by 20 kJ mol⁻¹, while for R = OMe the TS corresponding to branched product is favored by 6 kJ mol⁻¹. Both

(27) Smith, A. In *Chemistry*; University of Warwick: Coventry, 2001.

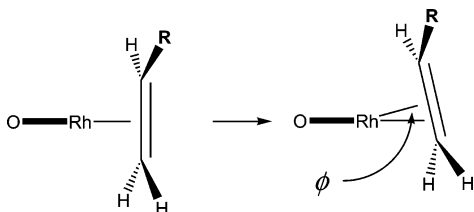


Figure 6. Definition of alkene roll angle in $[(\text{alkene})_2\text{Rh}(\text{acac})]$ complexes. See ref 26.

results are consistent with experiment. The TS structures closely resemble those for the cationic path with respect to the vinyl–alkene interaction. The distance between the two coupling carbon centers falls between 2.04 and 2.10 Å.

The next step would be to compute the TSs for $\text{R} = \text{CH}_2\text{-(OH)}$ for both cationic and anionic pathways to see whether the relative TS energies invert. However, before carrying out these calculations, we note that the small variation in barrier height for a given combination of R group and regiochemistry (Figure 3) indicates that the fate of the reaction is already implicit in the electronic structure of the reactant Pd complex. Hence, we first set about finding what feature(s) of the ground-state geometric and/or electronic structure might correlate with the regiochemistry.

Previous experimental and theoretical studies of the ground-state structures of Rh bisalkene complexes suggest a relationship between the alkene coordination geometry and the electronic nature of the olefin substituent.²⁶ Electron-donating substituents give a positive roll angle, ϕ (Figure 6), while electron-withdrawing groups give a negative ϕ . The present Pd species do not follow the same trend. For example, the roll angles for $[\text{Pd}(\text{dppm})(\eta^1\text{-CHCH}_2)(\eta^2\text{-CH}_2\text{CHOCH}_3)]^+$ and $[\text{Pd}(\text{dppm})(\eta^1\text{-CHCH}_2)(\eta^2\text{-CH}_2\text{CHCN})]^+$ are both positive (4.2° and 6.6°, respectively). In fact, for the substituents studied here, the ground-state structures of almost all the Pd complexes, whether neutral or cationic, have *positive* ϕ values.

Of course, olefin coordination is quite flexible and rotation around the metal–olefin centroid direction and displacements perpendicular to the coordination plane are relatively facile. So, if the key to the Heck reaction regiochemistry is not in the geometrical structure, perhaps it can be found in the electronic structure.

Following Tsipis,²⁸ simple perturbation theory for the reaction between two species A and B to form the molecule AB gives the following expression for the interaction energy, ΔE :

$$\Delta E = -\frac{q_r q_s}{R_{rs} \epsilon} + 2 \sum_m^{\text{occ}} \sum_n^{\text{unocc}} \frac{(c_r^m c_s^n \beta_{rs})^2}{E_m - E_n} \quad (1)$$

The bond is formed using the orbitals on atom r of A and s of B. The leading electrostatic term involves the atoms, with charges q_r and q_s , respectively, separated by a distance R_{rs} with ϵ the dielectric constant. The orbital term involves a summation over the occupied and unoccupied orbitals with the c_r^m coefficient describing the contribution from atom r to the m th occupied orbital of energy E_m while the c_s^n coefficient describes the contribution from atom s to the n th unoccupied orbital of energy E_n . The resonance integral between the two centers is given by β_{rs} .

(28) Tsipis, C. A. *Coord. Chem. Rev.* **1991**, *108*, 163–311.

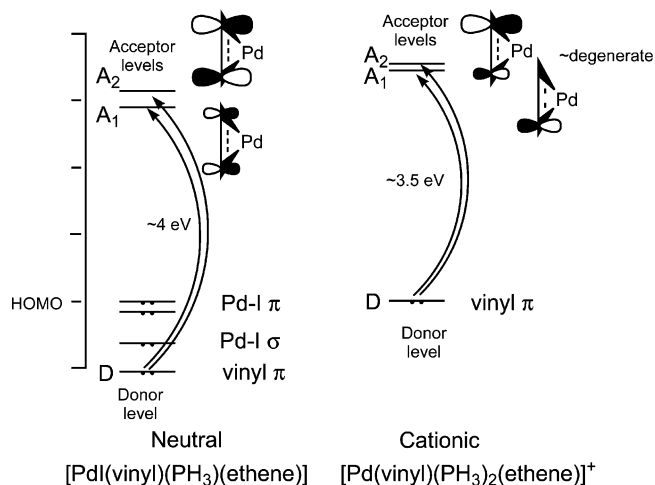


Figure 7. Schematic orbital energy level diagram for neutral and cationic ethene complexes adjusted to give HOMOs at the same energy.

In the present case, we consider the intramolecular C–C coupling as a nucleophilic attack on the alkene π system by the σ -bonded vinyl group. In the simplest possible scenario, there would be a single occupied donor MO with substantial vinyl character combining with a single empty acceptor MO located mainly on the alkene. However, the electronic structure of the planar reactant complexes (neutral and cationic) is more complicated.

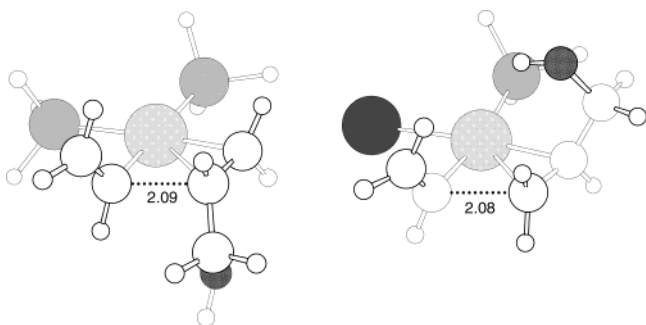
A schematic representation of the MO energy levels for the ethene complexes $[\text{PdI}(\text{vinyl})(\text{PH}_3)(\eta^2\text{-C}_2\text{H}_4)]$ and $[\text{Pd}(\text{vinyl})(\text{PH}_3)_2(\eta^2\text{-C}_2\text{H}_4)]^+$ is shown in Figure 7. For the cationic complex, the donor level, D, is also the HOMO while for the neutral complex the donor level lies below the Pd–I σ - and π -type MOs. However, the far more significant observation is that the LUMO and the LUMO+1 correspond to acceptor levels A_1 and A_2 and have significant contributions (20–40%) from the olefin π antibonding function (the orbitals in the cationic species are virtually degenerate and should be considered combined together). Once a substituent is placed on the olefin, each orbital tends to localize on one of the olefin carbons and, significantly, each orbital tends to localize on a *different* carbon. This has a critical effect on the predicted regiochemistry.

In eq 1, atom r is always the vinyl α carbon, C_{vin} . To a first approximation the charge on C_{vin} , ϵ , and the distance R_{rs} are nearly constant so that the first term in eq 1 is proportional to the charge on the alkene carbon. The electrostatic contribution to the regiochemical selectivity is thus proportional to the difference in alkene carbon atomic charges, $q(\text{C}_\alpha) - q(\text{C}_\beta) = \Delta q$. Similarly, given that the donor MO is constant, the orbital part of eq 1 is only affected by changes in the acceptor-orbital coefficients. Since these are squared (eq 1), the interaction becomes proportional to the percentage component, P , from a given alkene carbon (percentage $\propto c_s^2$) divided by the difference between the donor orbital energy, E_D , and acceptor orbital energies, E_{A1} or E_{A2} . Thus, the orbital contribution to the regiochemical selectivity is proportional to the difference between the percentage contributions from C_α and C_β for each acceptor orbital divided by the relevant donor–acceptor orbital energy difference. That is:

$$\Delta E_{\text{orb}} = (P_{\alpha 1} - P_{\beta 1})(E_{A1} - E_D) + (P_{\alpha 2} - P_{\beta 2})(E_{A2} - E_D) \quad (2)$$

Table 2. Electrostatic (a.u.) and Orbital Contributions (eV) to the Regioselectivity. A Positive ΔE_{orb} or $\Delta\rho$ Indicates Favorable Attack at the α Carbon To Give Branched Product

R	obsd regiochemistry	$\rho(C_\beta)$	$\rho(C_\alpha)$	$E_{\text{orb}}(\text{lin})$	$E_{\text{orb}}(\text{br})$	ΔE_{orb}	$\Delta\rho$
CN/cationic	linear	0.16	0.02	9.18	7.27	-1.91	-0.14
CN/neutral	linear	0.10	-0.05	10.54	6.84	-3.70	-0.15
OMe/cationic	branched	-0.01	0.58	3.84	5.71	1.87	0.59
OMe/neutral	branched	-0.02	0.47	6.46	7.55	1.10	0.49
CH ₂ (OH)/cationic	branched	0.15	0.16	5.66	6.81	1.15	0.01
CH ₂ (OH)/neutral	linear	0.10	0.08	8.33	7.88	-0.45	-0.02
Me/cationic	mixed	0.14	0.16	4.79	4.96	0.17	0.02
Me/neutral	mixed	0.10	0.08	7.71	7.57	-0.14	-0.02

**Figure 8.** Optimized TS structures for cationic (left) and neutral (right) pathways for R = CH₂OH.

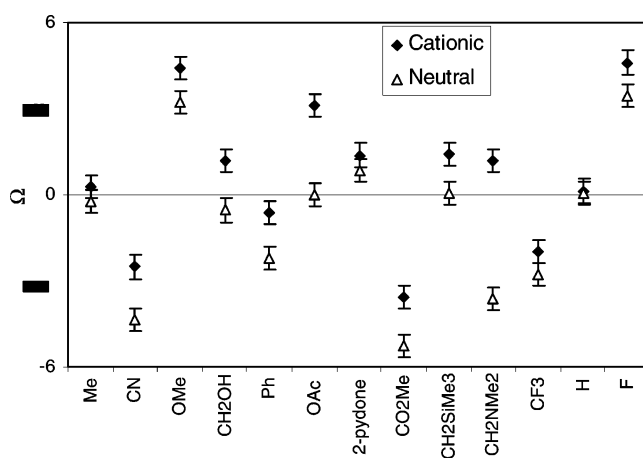
The first term in eq 2 thus describes the tendency for the A1 orbital to direct the regiochemistry while the second term describes the tendency for A2 to direct the regiochemistry.

The data in Table 2 show the results of computing electrostatic and orbital contributions to the attack at the α carbon to give branched product, or the β carbon to give linear product. The electrostatic term favors the most positive carbon center with $\Delta q = q(C_\alpha) - q(C_\beta) > 0$ indicating branched product. Similarly, a positive difference between the orbital terms for each carbon center favors branched product.

For all four R groups in Table 2, the charge and orbital terms act in the same sense and reinforce each other. For R = CN and OMe the regiochemistry is the same for both cationic and neutral pathways and so are the signs of ΔE_{orb} and Δq , while for R = CH₂OH the observed change in regiochemistry is accompanied by a change in the signs of ΔE_{orb} and Δq for each pathway. The signs of ΔE_{orb} and Δq also change for R = CH₃, but their magnitudes are small. Thus, we can predict the general regiochemical outcome of the reaction directly from the precursor compound. Moreover, these results, particularly for R = CH₂OH, demonstrate that the regiochemistry cannot be predicted solely from a scale of substituent effects based on the isolated olefins since such a scale would not allow for the regiochemistry to be changed by the reaction conditions. The chemistry is profoundly influenced by binding to the palladium center and this interaction must be explicitly accounted for.

To confirm the qualitative predictions for R = CH₂OH, the actual TSs for the four relevant pathways were optimized. As expected, the branched TS for the cationic pathway is 10.5 kJ mol⁻¹ lower than for linear (Figure 8, left), while for the neutral pathway the linear path TS is 12.3 kJ mol⁻¹ lower (Figure 8, right). Hence, the ground-state prediction is faithfully reproduced by the TS calculations.

In order to derive a more quantitative descriptor, the charge and orbital contributions need to be scaled. The parent system

**Figure 9.** Comparison of computed selectivity numbers and experimental product distributions (linear/branched). An uncertainty of ± 0.4 is shown by vertical bars on each point.**Table 3.** Theoretical Selectivity Numbers Compared to Experimental^{9,30} Product Ratios

R	$\Omega(\text{cationic})$	selectivity (% lin/ % br)	$\Omega(\text{neutral})$	selectivity (% lin/ % br)
F	4.61		3.45	
OMe	4.43	0/100	3.22	30/70
OAc	3.10	5/95	0.00	mix
CH ₂ SiMe ₃	1.40		0.06	
2-pydone	1.39	0/100	0.83	60/40
CH ₂ NMe ₂	1.21		-3.60	
CH ₂ OH	1.19	0/100	-0.54	100/0
Me	0.26	20/80	-0.23	80/20
H	0.14	—	0.08	—
Ph	-0.60	60/40	-2.23	100/0
CF ₃	-2.00		-2.78	
CN	-2.52	100/0	-4.35	100/0
CO ₂ Me	-3.58	100/0	-5.25	100/0

with R = H is unsuitable for this since the electrostatic and orbital terms are close to zero. Instead, we chose to scale the two terms with respect to R = OAc under neutral conditions since this reaction is reported to give a mixture of products. The computed Δq term for R = OAc was scaled relative to ΔE_{orb} to give a total interaction energy of zero. This corresponds to multiplying the charge term by 4.3 and defines a selectivity index, Ω , which measures the tendency for a given R group to direct attack at the adjacent C_α carbon ($\Omega > 0$) or at the remote C_β carbon ($\Omega < 0$) (eq 3). Values for Ω are plotted in Figure 9 and given in Table 3 along with experimental product ratios for the comparable arylation reactions. Details of how these data were computed are provided in the Supporting Information. Note that since Ω relies on partial atomic charges and orbital composition which here are computed by a Mulliken analysis of the LDA charge distribution, the detailed form of eq 3 is

$$\Omega = \Delta E_{\text{orb}} + 4.33\Delta q \quad (3)$$

specific to the chosen basis set/method combination. However, we presume that other sources of atomic charges and orbital energies and compositions can be put into the same form, providing that calculations on a few of the systems described here are repeated to establish the scaling relationships between our ΔE_{orb} and Δq terms and those derived from other theoretical results.

Although the experimental product ratios may not always be quantitatively reliable, it is remarkable how consistent the

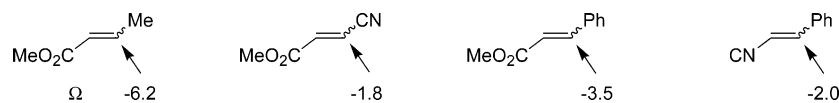


Figure 10. Compound selectivity numbers for disubstituted alkenes relative to left-hand substituent. The arrow indicates the experimental coupling position.

qualitative agreement between theory and experiment is. When Ω is negative the remote β carbon is attacked, leading to linear product, while for positive Ω the α carbon is attacked, leading to branched product. When Ω is close to zero, a mixture of products is predicted and usually observed. The threshold values at which the selectivity becomes complete differ for cationic versus neutral pathways. For cationic conditions, a mixture of products is predicted for $-0.6 < \Omega < 0.3$, while under neutral conditions, a mixture results for $\Omega > -0.2$. For the R groups in Table 3, there are apparently no examples of complete selectivity for branched product so no upper limit on Ω can be specified.

These ranges are of the order of the uncertainty in Ω values which is itself dominated by the orbital term ΔE_{orb} . An error of 1% in the percentage contributions in the acceptor orbitals, coupled with the donor–acceptor energy difference of 3.5 to 4 eV, results in a variation in Ω values of $\sim 1/4 - 1/3.5 = 0.25 - 0.3$. The effect of errors in the Mulliken charges is much smaller. An uncertainty in the charges of 0.02 results in a change in Ω of 0.08. Overall, the Ω values are probably only reliable to about 0.4 which is reflected in the error bars attached to the data points in Figure 9.

A significant conclusion of the present study is that no single component of the interaction energy yields consistent predictions of regioselectivity and all three contributions to ΔE are required. Previous reports of correlations between regiochemistry and LUMO coefficients apply only to a restricted set of substituents and reaction conditions.²⁹

Since Ω is based on a Mulliken analysis of the charges and MO compositions, the actual numerical values will depend on the basis set. However, by following the procedures described in the Supporting Information, it should be possible to map a different choice of computational scheme onto the present scale of Ω values.

The selectivity numbers appear to provide a purely *electronic* basis for rationalizing the regiochemistry of intermolecular Heck couplings. Note that the DFT calculations were based on a relatively simple geometry optimization of the precursor *vinyl* complex but that the experimental data refer to *arylations*. The bulkiness of the aryl group has been invoked to explain the tendency for coupling to the less hindered β carbon under neutral reaction conditions. While most of the Ω values are indeed negative, there are some notable exceptions such as OMe. Apparently, electronic effects are more important than steric interactions which is not unexpected given the TS structures in Figures 3, 5, and 8. The steric interactions do not look like they would be substantially altered if vinyl were replaced by a phenyl group. Moreover, sample calculations where vinyl is replaced by phenyl give virtually identical charges and orbital compositions on the olefin carbons. This is not to say that sterics play no role at all, rather that for the R groups of this study whatever steric interactions occur are of secondary importance.

Another significant feature of the data in Figure 9 concerns the prediction of α attack under cationic conditions for R = CH_2SiMe_3 ³¹ and CH_2NMe_2 .³² This regiochemistry is observed for arylation reactions but, in the case of the amine, the

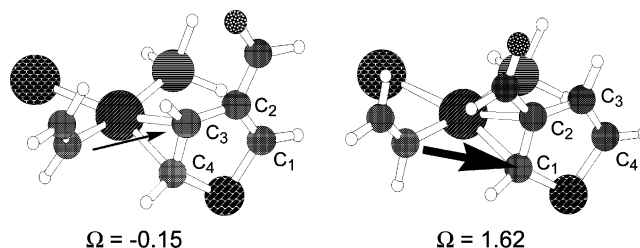


Figure 11. Optimized structures for thiophene-3-carboxaldehyde complexes.

regiochemistry was attributed to secondary Pd–N coordination.³² While the present calculations cannot discount such an interaction playing a role somewhere along the reaction pathway, there is no evidence of any such interaction in the ground-state structure of the precursor and, given the positive Ω values, the observed regiochemistry can be explained simply as arising from the electronic consequences of binding the allylamine or allyltrimethylsilane to the Pd center. For the amine, the model predicts the reverse regiochemistry for neutral reaction conditions. This would be an interesting test of the theory but, to our knowledge, has not been reported.

The Ω values are roughly additive so that they can also be used to predict the regiochemistry when two substituents are in competition. Thus, for alkenes of general formula RCHCHR' , DFT calculations under neutral pathway conditions predict the selectivities shown in Figure 10. The directly calculated values -6.2 , -1.8 , -3.5 , and -2.0 compare reasonably well with those derived from adding the relevant values from Table 3, viz. -5.0 , -0.9 , -3.0 , and -2.1 , respectively. The predicted sites of attack are consistent with experiment.³³

A roughly 1:2 mixture of products is reported for the arylation of ethyl (*E*)-4,4,4-trifluorocrotonate.³⁴ Substitution at the carbon α to the ester substituent is preferred which runs counter to the predictions based on the Ω values. Since $\Omega(\text{CO}_2\text{Me})$ is more negative than $\Omega(\text{CF}_3)$ under both cationic and neutral conditions, arylation is predicted to occur α to the CF_3 group. However, this discrepancy may not be significant since the isolated yields are low (~ 20 to 50%).

Finally, we considered the reaction between thiophene-3-carboxaldehyde and iodobenzene.³⁵ Assuming neutral conditions, the optimized geometries were computed for coordination via each double bond. To maintain consistency with the rest of the paper, Figure 11 shows the computed structures for the vinyl species. However, the conclusions are identical for the phenyl analogues.

- (29) Shmidt, A. F.; Vladimirova, T. A.; Shmidt, E. Y. *Kinet. Catal.* **1997**, *38*, 245–250.
- (30) Cabri, W.; Candiani, I.; Bedeschi, A.; Santi, R. *J. Org. Chem.* **1992**, *57*, 3558–3563.
- (31) Olofsson, K.; Larhed, M.; Hallberg, A. *J. Org. Chem.* **1998**, *63*, 5076–5079.
- (32) Olofsson, K.; Larhed, M.; Hallberg, A. *J. Org. Chem.* **2000**, *65*, 7235–7239.
- (33) Littke, A. F.; Fu, G. C. *J. Am. Chem. Soc.* **2001**, *123*, 6989–7000.
- (34) Gong, Y. F.; Kato, K.; Kimoto, H. *J. Fluorine Chem.* **2000**, *105*, 169–173.
- (35) Lavenot, L.; Gozzi, C.; Ilg, K.; Orlova, I.; Penalva, V.; Lemaire, M. *J. Organomet. Chem.* **1998**, *567*, 49–55.

The Ω values computed relative to the sulfur are shown at the bottom of Figure 11. Although the left-hand isomer is ~ 11 kJ mol⁻¹ more stable, if we continue to assume the Curtin-Hammett postulate, then the regiochemistry is determined by the largest Ω value which corresponds to attack at the carbon center between the sulfur and the aldehyde substituent, C₁. Although up to 40% of the reaction leads to biphenyl, the distribution of the products from the thiophene arylation favors attack at C₁ by a factor between 4 and 14, in general agreement with the theoretical prediction.

Conclusions

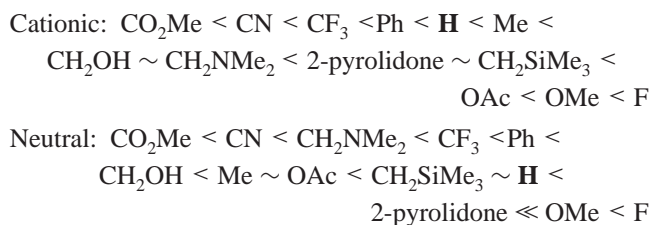
DFT calculations of the reaction paths for the Heck coupling of a vinyl group with various monosubstituted alkenes show that the transition-state structures and reaction barriers are relatively insensitive to the exact placement of the alkene substituent but do depend significantly on the regiochemistry. This conclusion is independent of the pathway and holds for both cationic [PdRL₂(alkene)]⁺ and neutral [PdRIL(alkene)] complexes (R = vinyl; L₂ = dppm; L = PH₃). These results imply that the basic regiochemistry is already implicit in the electronic structure of the precursor metal complexes.

Accordingly, a simple selectivity index, Ω , has been developed solely on the basis of the electronic structure of the optimized precursor Pd complex which quantifies the tendency for a given alkene substituent, R', to direct the incoming R group (vinyl or aryl) to either the adjacent carbon, C_α ($\Omega > 0$), or the remote ($\Omega < 0$) carbon, C_β. This selectivity index has an electrostatic component which depends only on the difference between Mulliken charges of the olefin carbon atoms, plus a *double* orbital component which depends on the compositions of *two* empty acceptor MOs with significant alkene components and their energy differences with respect to a single filled donor MO with a substantial contribution from the vinyl donor atom.

The selectivity index is derived from the geometry optimization of the precursor Pd complex and can readily be extended to other alkene substituents to provide the basis for a more rational approach to the use of the intermolecular Heck reaction where steric effects are minimal. Once scaled to produce a 50/50 product distribution for R' = OAc under neutral conditions, the Ω values correctly predict the regiochemistry under both neutral and cationic intermolecular Heck coupling conditions for a range of R' groups. In particular, Ω predicts the

regiochemistry should reverse for R = CH₂OH, which was confirmed by explicit TS optimizations, and suggests that secondary interactions from R groups containing amine or silyl centers are not required to explain experiment.

The order of the Ω values for cationic and neutral conditions is:



In each case, groups to the left of H direct R to the β carbon while those to right tend to direct R to the α carbon.

The Ω values are approximately additive and generally predict the correct regiochemistry for disubstituted alkenes where the two substituents are in competition. For cyclic thiophene-3-carboxaldehyde which contains two olefin bonds, the observed site of attack agrees with the predicted site based on the largest Ω value.

This study complements that of von Schenck et al.¹⁵ in that they explored the regiochemistry as a function of auxiliary ligand but with a single olefin. Here, we have looked at two generic types of auxiliaries (two phosphines and a phosphine/halide combination) and a wide range of olefins. Provided that the same procedure is adopted as described here, the atomic charges, MO compositions, and MO energies derived from other basis set/functional combinations could be employed and by using some of the R groups reported here, new Ω values can be mapped onto the present Ω scale. Future work will be directed to examining whether the Ω selectivity index can be extended to diimine and mixed N,O donor systems and augmented to account for steric effects.

Acknowledgment. R.J.D. acknowledges the support of the EPSRC.

Supporting Information Available: Raw data used to compute Ω and an explicit example of its calculation. This material is available free of charge via the Internet at <http://pubs.acs.org>.

JA0315098